Journal of Fluids and Structures (2002) **16**(1), 83–92
doi:10.1006/jfls.2001.0404, available online at http://www.idealibrary.com on IDEAL®

THE CROSSING FREQUENCY AS A MEASURE OF HEAT EXCHANGER SUPPORT-PLATE EFFECTIVENESS

M. K. Au-Yang

3531 Round Hill Road, Lynchburg, VA 24503, U.S.A.

(Received 15 July 2000, and in final form 13 March 2001)

The crossing frequency is the number of times per second the vibration amplitude crosses the zero displacement line from negative displacement to positive displacement. In flow-induced vibration in which the motions are often random and/or a number of modes contribute to the vibration amplitudes, the crossing frequencies are modal-weighted average frequencies of the vibration. It is postulated in this paper that the crossing frequency can be used as a measure of heat exchanger support-plate effectiveness. Using a time-domain, nonlinear analysis technique, the crossing frequencies of a tube vibrating in support plates with oversized holes can be computed as a function of time and the tube-to-support-plate clearances. It was found that the fluid–elastic stability margin of a tube bundle, in the context of the original Connors' equation for tube bundle fluid–elastic instability, should be independent of the tube-to-support-plate clearances. A simple method of estimating the critical velocity based on the time-domain equation of fluid–elastic stability is suggested.

1. INTRODUCTION

It is well known that as the cross-flow velocity across a closely packed tube bundle increases beyond a certain value, called the critical velocity, the tube bundle will become unstable. The motion of the tubes changes from individually random to organized orbital, with amplitudes rapidly increasing as the cross-flow velocity increases, until tube-to-tube impacting occurs. Based on a combination of experimental data derived from tests on a row of flexibly supported, single-span tubes subjected to uniform cross-flow, and phenomenological reasoning, Connors (1970, 1978) deduced the following equation for determining the critical velocity:

$$V_c = \beta f_n \sqrt{\frac{2\pi\zeta_n m_t}{\rho}}. \tag{1}$$

Since $m_t(2\pi f_n)^2 = k_n$, the modal or generalized stiffness, the critical velocity for a particular mode is completely governed by the modal stiffness of the tube.

Since Connors first discovered this phenomenon, refinements on the above basic equation to account for the effect of nonuniform velocity and density distributions, tube bundles involving more than one row of tubes, tube bundles involving more than one span of tubes, and tube bundles of different pitch-to-diameter ratios and of different arrangements have been given by many authors. Like Connors' original equation, nearly all of these later "refinements" are basically frequency-domain equations. A review paper by Price (1993), together with the extensive bibliography it contains, gives further details on the general subject of tube bundle fluid–elastic instability. The objective of this paper is to address the

0889–9746/02/010083 + 10 $35.00/0

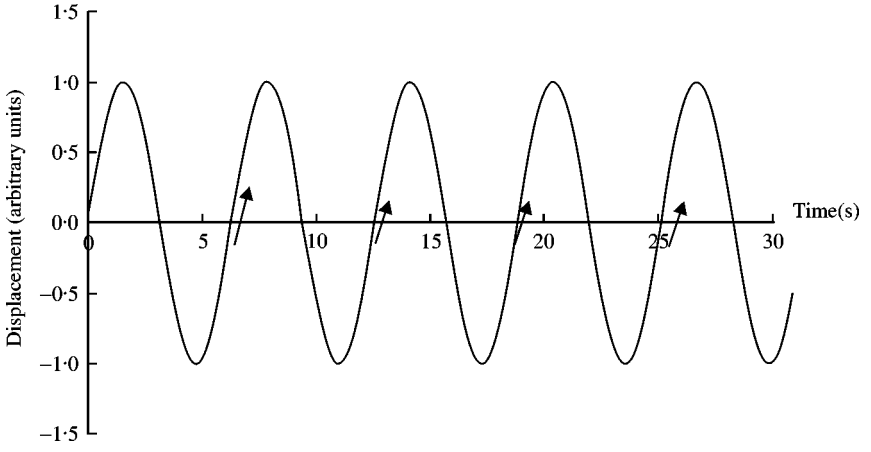

Figure 1. In a structure vibrating in one mode, the positive crossing (arrows) frequency is equal to its modal frequency.

other questions: what is the effect of finite tube-to-support-plate clearance on the critical velocity as predicted by the Connors equation, and how can the critical velocity in an industrial heat exchanger be more correctly predicted with the time-domain, nonlinear formulation of tube bundle fluid–elastic stability? To answer these questions, we apply a concept that is commonly used in fatigue analysis—the crossing frequency.

2. THE CROSSING FREQUENCY

The crossing frequency, or more accurately the positive crossing frequency, is defined as the number of times per second the response (displacement, stress, strain, etc.) at a point of a structure crosses the zero (or mean, if there is a static mean) response line from the negative amplitude to the positive amplitude. In a linear structure vibrating in one mode, the crossing frequency is equal to the modal frequency of the structure, as shown in Figure 1. In a linear structure vibrating with more than one mode, it can be shown that (Rice 1944, 1954; Crandall & Mark 1973) the crossing frequency is an effective modal-participation-weighted mean frequency of the structure:

$$f_c^2 = \frac{\int_0^\infty f^2 G_d(f)\,\mathrm{d}f}{\int_0^\infty G_d(f)\,\mathrm{d}f}. \tag{2}$$

As shown in Figure 2, if the structure vibrates predominantly in the first mode, its crossing frequency will be almost equal to its first modal frequency, while if it vibrates predominantly in the second mode, its crossing frequency will be almost equal to its second modal frequency. If both modes contribute equally to the response, its crossing frequency will be a weighted average of these two frequencies. Figure 3 shows the crossing frequency of a heat exchanger tube with oversized tube support-plate holes. The motion in this case is chaotic.

The crossing frequency concept has been used by engineers to predict the fatigue usage of structural components vibrating with a combination of normal modes, based on fatigue curves derived from tests using cyclic loads, each at one specific frequency. Since the modal frequency is a measure of the stiffness of the structure vibrating in that particular mode, and the crossing frequency is a modal-participation-weighted average of the modal frequencies, one can deduce that the crossing frequency is a modal-participation-weighted measure of

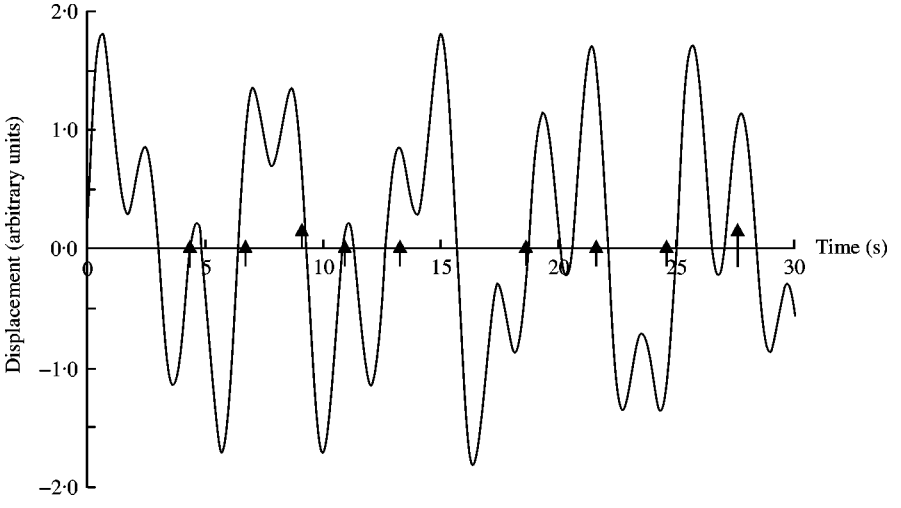

Figure 2. A structure vibrating in two modes, the positive crossing (arrows) frequency is a modal-participation-weighted average of the two modal frequencies.

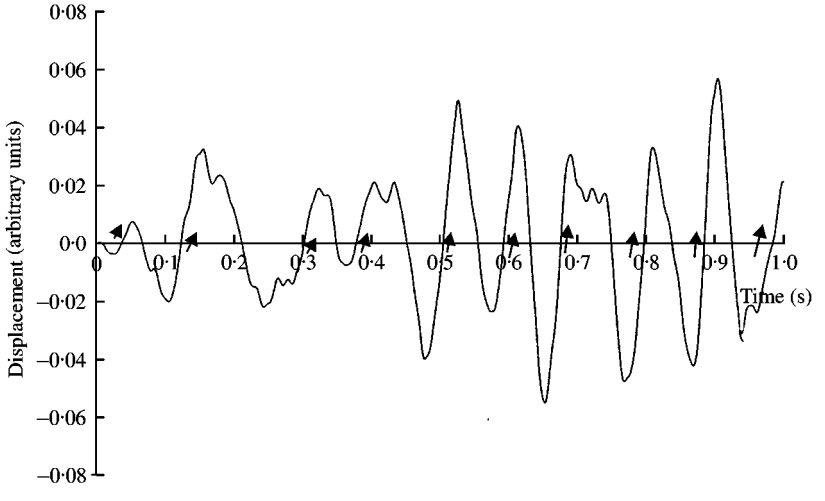

Figure 3. Crossing frequency of a system undergoing chaotic motion.

the system stiffness of the structure, vibrating in a combination of normal modes. Since in Connors' equation (1), the modal critical velocity is completely governed by the tube modal stiffness, it is reasonable to assume that when more than one mode becomes unstable at the same time, the system critical velocity (instead of the modal critical velocity) would be completely governed by the system stiffness (or crossing frequency) of the tube.

3. A TIME-DOMAIN EQUATION FOR THE CRITICAL VELOCITY

In the time domain, the equation of motion for a tube in a tube bundle can be written as

$$M\ddot{y} + (C_{\text{sys}} + C_{\text{FSI}})\dot{y} + ky = F_{\text{ext}}. \tag{3}$$

By assuming a "velocity-controlled" fluid–structure interaction mechanism, Chen (1983), Axisa (1988) and Sauvé (1996) show that

$$C_{\mathrm{FSI}} = 4\pi M f_o \zeta_{\mathrm{FSI}} \quad \text{and} \quad \zeta_{\mathrm{FSI}} = -\frac{\rho V_p^2/2}{\pi f_o^2 m \beta^2}, \tag{4}$$

and equations (3) and (4) together reduce to the form of Connors' equation (1). The remaining question is, what is f_o?

Axisa used the modal frequency f_n for f_o, defeating the purpose of writing the stability equation in the time domain, with the objective of nonlinear analysis in which the very concept of normal modes can no longer be used. Sauvé (1996) called f_o a participation frequency and computed and updated it at every time step in the solution. As Sauvé put it, the major task of the entire procedure was to compute this "participation frequency". The need to continually update this frequency resulted in a very time-consuming algorithm. It is postulated in this paper that in equation (3), f_o is the crossing frequency f_c. In terms of the crossing frequency, Connors' equation can be written as

$$V_c = \beta f_{cc} \sqrt{\frac{2\pi \zeta_{\mathrm{sys}} m_t}{\rho}}, \tag{5}$$

where f_{cc} is the crossing frequency at the threshold of instability and the system "damping ratio" is related to the system damping coefficient by

$$C_{\mathrm{sys}} = 4\pi M f_{cc} \zeta_{\mathrm{sys}}. \tag{6}$$

Note that ζ_{sys} does not include damping due to fluid–structure interaction.

Being a frequency-domain parameter, the "participation frequency" is difficult to compute in a nonlinear time-domain analysis. The crossing frequency, on the other hand, is a time-domain parameter. With today's computing software and hardware, the crossing frequency can readily be obtained by actually *counting* the number of times per second the response crosses the zero (or mean, if there is a static mean) axis from the negative to the positive. Provided that Connors' constant and the crossing frequency are approximately constant as a function of the tube-to-support-plate clearance, the critical velocity can then be obtained as a function of the tube-to-support-plate clearance.

4. NUMERICAL EXPERIMENT

A tube in a large commercial nuclear steam generator (Figure 4) was used to study the effect of tube-to-support-plate clearance on the crossing frequency, and hence on fluid–elastic loading, during normal operations (below the critical velocity) and as the velocity increased beyond the critical velocity. A frequency-domain linear analysis (that is, without tube–support-plate clearances) was carried out first. The forcing function was obtained by fitting an upper-bound curve to the two-phase power spectral density data of Pettigrew & Taylor (1993). The reaction forces at the top support plates and the r.m.s. displacement at the apex were computed. For the nonlinear time-domain analysis with tube–support-plate clearances, two point loads, each with an in-plane and an out-of-plane component, were applied to the U-bend of the steam generator tube to simulate the distributed turbulence-induced forcing function. The spectral shapes of these point loads were taken to be the same as the above-mentioned empirical upper bound curve to the two-phase spectrum, while its magnitudes were adjusted until they gave the same reaction forces at the top support plates of the tube, and about the same r.m.s. displacement at the apex of the U-bend. Based on the reasonable assumption that the wear rate between the tube and the support plate depends

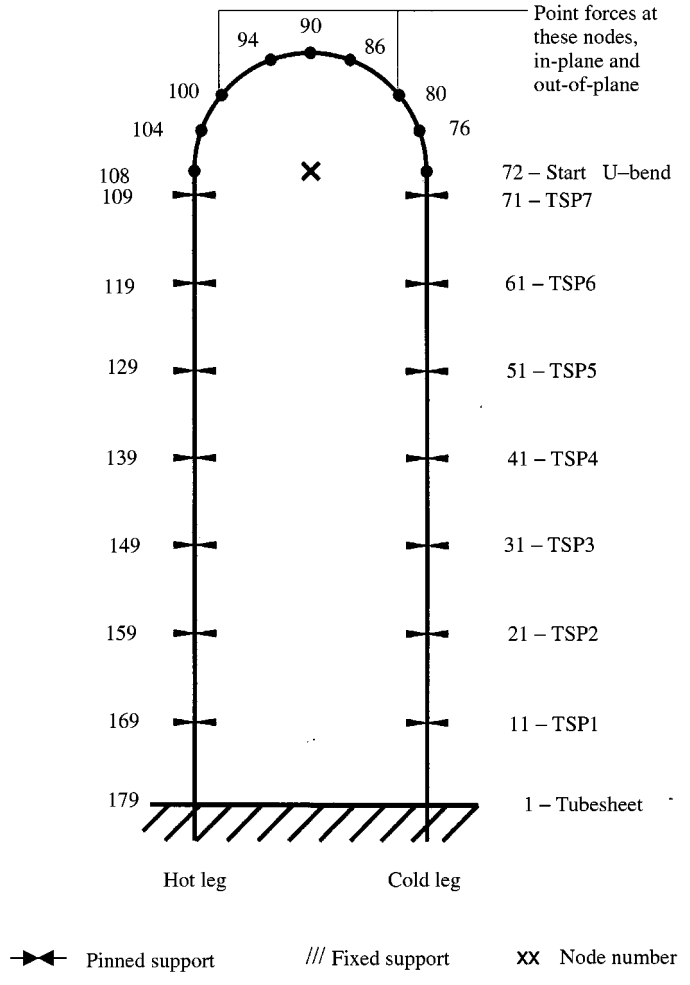

Figure 4. Finite-element model of nuclear steam generator tube under study. To simplify the time-domain nonlinear analysis, the distributed random pressure force was replaced by two random point forces, F1 and F2, each with an in-plane and an out-of-plane component. The magnitudes of these two point forces were adjusted to give approximately the same vibration amplitude at the apex and the same reaction forces at the top support plates (nodes 71 and 109), as those caused by the distributed random pressure: →←, pinned support; ///, fixed support; ××, node number.

only on the reaction force at this support plate and the displacement at the apex of the U-bend, these two point loads were used in subsequent time-domain wear work-rate calculations for the tube. This approach greatly reduced the computation time for this nonlinear wear analysis.

These two frequency-domain point loads were then transformed into two time-domain point loads by inverse fast Fourier transform (FFT). These were substituted into the right-hand side of equation (3) and a nonlinear finite-element computer program was used to solve the equation, with and without clearances between the tube and the tube support plates. The following cases were considered.

(i) *Normal operation condition* (tube stable, cross-flow velocity equal to half the critical velocity). Solutions for 0, 1, 2 and 3 times the normal tube-to-support-plate clearance were

Gap	Crossing frequencies (Hz)	
0	20·3	20·3
1×	16·5	19·3
2×	9·3	19·6
3×	7·0	19·3

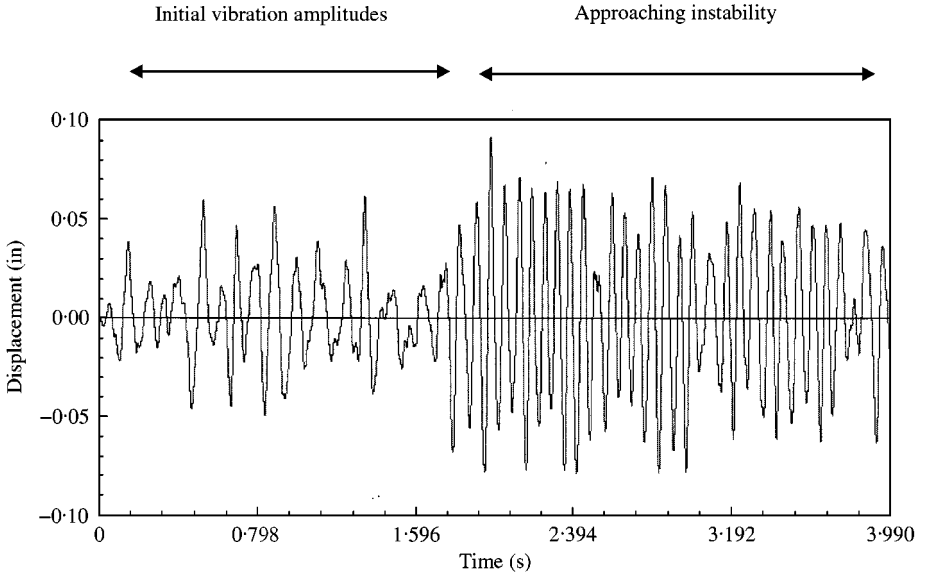

Figure 5. Initial crossing frequency versus crossing frequency as the tube approaches the instability threshold (1 in = 25·4 mm).

obtained for 4·0 s. The crossing frequencies were computed as a function of time in each case.

(ii) *Behavior near instability threshold*. The negative damping force due to fluid–elastic coupling (C_{FSI}) in equation (3) was gradually increased until the tube became unstable. Again 4.0 s of solution was obtained in each case and the crossing frequencies were computed as a function of time.

5. RESULTS

Figure 5 shows the out-of-plane (z-direction) time history response at the apex of the U-bend, when the tube-to-support-plate clearances are 0 (i.e., linear case), 1, 2, and 3 times the as-built nominal clearance. The fluid–elastic force C_{FSI} on the left-hand side of equation (3) was adjusted in each case so that the tube was just at the instability threshold. Also shown in Figure 5 are the initial crossing frequencies when the vibration amplitudes were small, and the crossing frequencies as the vibration amplitudes started to grow and the system approached instability. In each case, 4·0 s of record is shown. Figure 5 shows that during the initial 1·5 s when the amplitudes were small, the crossing frequencies depended on the tube-to-support-plate clearances. As the vibration amplitudes grew and the tube

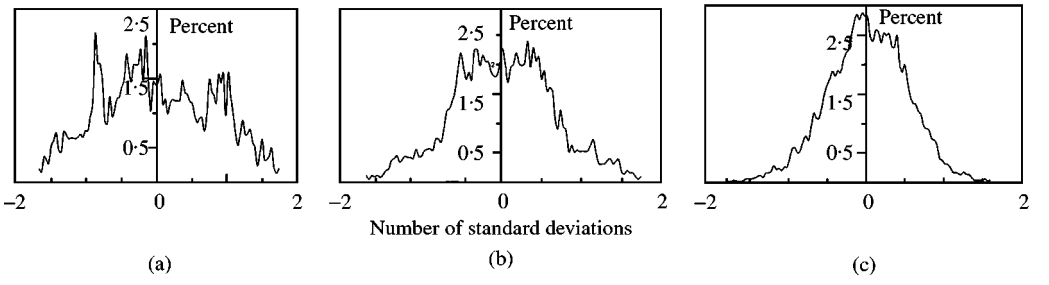

Figure 6. Amplitude probability distribution plots of a loosely supported tube: (a) below the critical velocity; (b) at the critical velocity; and (c) that of a tube without tube–support-plate clearance.

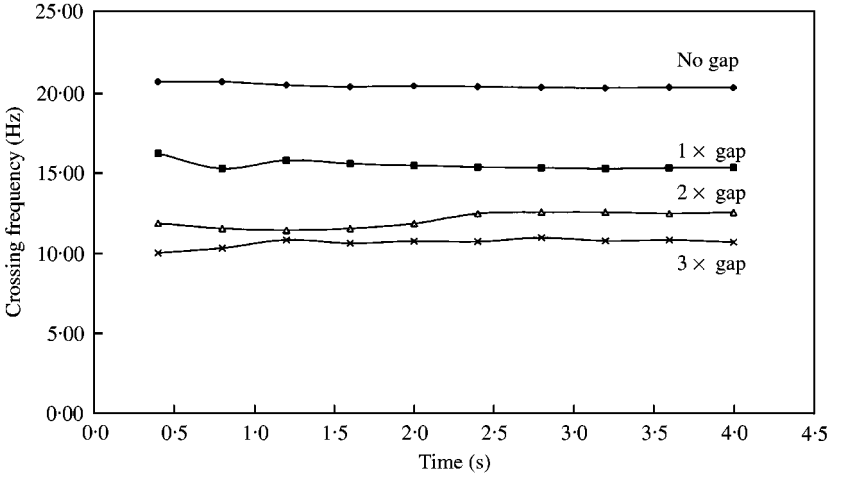

Figure 7. Crossing frequencies as a function of time for different tube–support-plate clearances (below the critical velocity).

approached instability, the crossing frequencies all approached that of a tube without tube-to-support-plate clearance.

Figure 6 shows amplitude probability distribution function (PDF) plots during the initial 1·5 s of the response, when the vibration amplitudes were small, and the final 2·0 s of the response, when the vibration amplitudes were large and the system was approaching instability. These PDF plots show that when the vibration amplitudes were small compared with the tube–support-plate clearance, the motion was "chaotic". However, as the instability threshold was approached and the vibration amplitudes increased, the motion started to "organize" itself and became more like random vibration, except within the boundary of the support-plate hole, where the motion was still chaotic. When the instability threshold was exceeded, the "flat top" regions of the PDF plots continue to "shrink" until the PDF plots approached those exhibited by a tube without tube-to-support-plate clearance (Gaussian random).

Figure 7 shows the crossing frequency as a function of time in each of the above cases with different tube-to-support-plate clearances, when the tube was under normal loading conditions (i.e., stable, but with fluid–elastic force). In all cases, the crossing frequencies were approximately constant except for the initial seconds of the response.

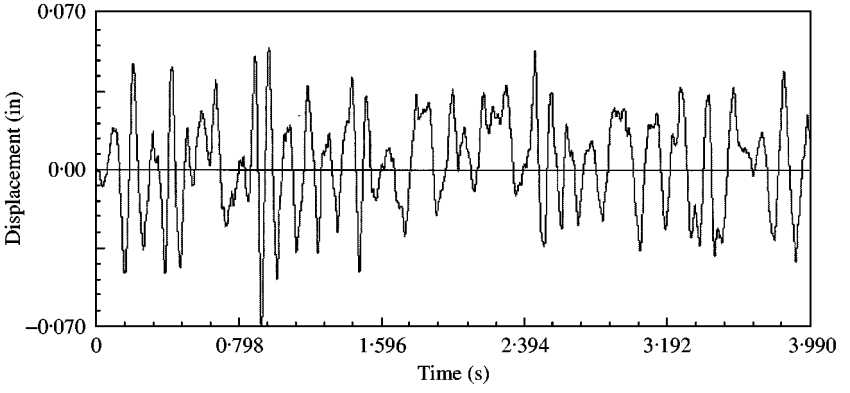

Figure 8. Details of chaotic motion before instability, 3 × clearance, at apex of a U-bend.

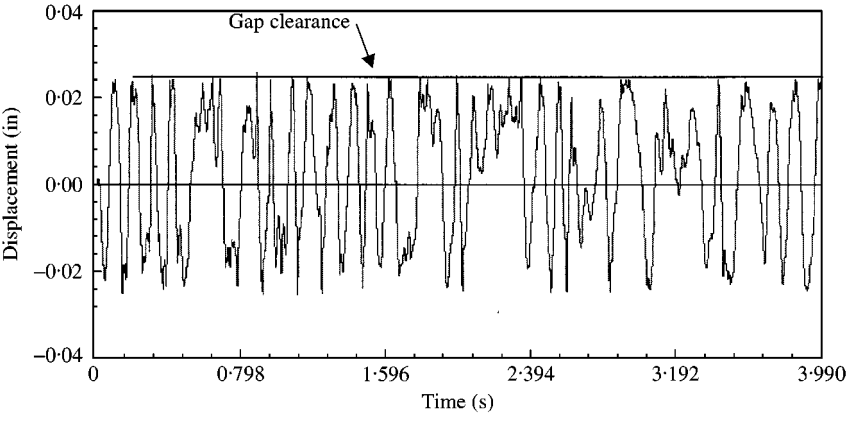

Figure 9. Details of motion at the top support plate showing that the support plate is active.

Figure 8 shows the out-of-plane time history response of a point at the apex of the U-bend, when the tube-to-support-plate clearance is 3 times the as-built nominal clearance.

Figure 9 shows the corresponding tube response at the top support plate, and shows that this support plate was active, even though the vibration amplitude at the apex was relatively small.

6. CONCLUSIONS

This study has shown the following.

1. Assuming fluid–elastic loading,

$$C_{\mathrm{FSI}} = -4\pi M f_c \frac{\rho V_p^2/2}{\pi f_c^2 m \beta^2} = -\frac{4qL}{f_c \beta^2} \quad \text{with} \quad q = \tfrac{1}{2}\rho V_p^2$$

exists (even below the critical velocity); this fluid–structure interaction effect can be implemented into a nonlinear time-domain equation either as a constant forcing function on the right-hand side of the equation, or as a negative damping on the left-hand side of the

equation. Once the crossing frequency is determined (by counting in the time domain) from the initial second or so of the solution, there is no need to update this fluid–elastic load in subsequent time steps. This results in tremendous saving of computation time. While the "velocity-controlled" fluid–structure interaction mechanism is used in this study as a specific example, the same conclusion applies to any other models of fluid–structure coupling, such as Chen's (1983) "fluid stiffness-controlled" model.

2. Effect of tube–support-plate clearance on instability threshold

As a tube becomes unstable, the crossing frequencies approach the same values as that for a tube without tube-to-support-plate clearance. Thus, the critical velocity, in the context of the original Connors' equation (1), with β constant, is independent of tube-to-support-plate clearance. Physically this is because as the amplitude approaches "infinity", the tube–support clearance becomes infinitesimal in comparison with the vibration amplitude, irrespective of its actual value. In practice, however, the tubes would hit each other long before their vibration amplitudes become "infinite". Thus, aside from instability and wear, one of the criteria in tube bundle dynamic analysis is that, as the gap clearance increases, the mid-span vibration amplitudes must be small enough so that frequent tube-to-tube impacting will not occur. This, however, can be solved by standard nonlinear time-domain analysis.

3. Support-plate effectiveness

Even well below the instability threshold, tube bundles built with normal tube-to-support-plate clearances vibrate with the support plates mostly active.

4. Critical velocity in the time-domain

The time-domain stability equations (3) and (4) can be used to predict the critical velocity in an industrial heat exchanger tube with multiple spans, closely spaced modal frequencies and tube-to-support-plate interactions, by gradually increasing the magnitude of C_{FSI} until the solution starts to diverge. Separate studies showed that using this method, the critical velocity is dependent on the tube–support clearance. Within the range of industrial interest, the critical velocity generally increases with tube–support clearance. This will be the subject of a future publication.

References

Axisa, F. *et al.* 1988 Overview of numerical methods for predicting flow-induced vibration. *ASME Journal of Pressure Vessel Technology* **110,** 6–14.

Chen, S. S. 1983 Instability mechanism and stability criteria of a group of cylinders subject to cross flow. Parts I and II. *ASME Journal of Vibration, Acoustics, Stress and Reliability in Design* **105,** 51–58 and 253–260.

Connors, H. J. 1970 Fluid–elastic vibration of tube arrays excited by cross flow. In *Flow-Induced Vibration in Heat Exchangers* (ed. D. D. Reiff), pp. 42–56. New York: ASME.

Connors, H. J. 1978 Fluid–elastic vibration of heat exchanger tube arrays. *ASME Journal of Mechanical Design* **100,** 347–353.

Crandall, S. H. & Mark, W. D. 1973 *Random Vibrations in Mechanical Systems.* New York: Academic Press.

Pettigrew, M. J. & Taylor, C. E. 1993 Two-phase flow-induced vibration. In *Technology for the 90s* (ed. M. K. Au-Yang). pp. 813–864. New York: ASME.

Price, S. J. 1993 Theoretical models of fluid–elastic instability for cylinder arrays subject to cross flow. In *Technology for the '90s*, (ed. M. K. Au-Yang). pp. 711–773. New York: ASME.

Rice, S. O. 1944, 1954 Mathematical analysis of random noise. *Bell System Technical Journal* **23,** 282–332, and **24,** 46–156.

Sauvé, R. G. 1996 A computational time domain approach to solution of fluid–elastic instability for non-linear tube dynamics. In *Flow-Induced Vibration-1966* (ed. M. J. Pettigrew) PVP-vol. 328, pp. 327–335. New York: ASME.

APPENDIX: NOMENCLATURE

C_{sys}	system damping coefficient
C_{FSI}	damping from fluid–elastic coupling
f_c	crossing frequency
f_{cc}	crossing frequency at instability threshold
f_n	modal frequency
$G_d(f)$	response power spectral density
k_n	generalized stiffness
L	length of the tube
$M = mL$	total mass of the tube
m_t	linear mass density of tube, including added mass and mass of water contained
V_c	critical velocity for instability
V_p	pitch velocity
β	Connors' constant
ζ_n	modal damping ratio
ζ_{FSI}	damping ratio from fluid–elastic coupling
ζ_{sys}	system damping ratio (of tube only)
ρ	shell side fluid density